JOURNAL OF THEORETICAL AND APPLIED MECHANICS
51, 1, pp. 63-73, Warsaw 2013

CONSTITUTIVE MODEL FOR TIME-DEPENDENT RATCHETTING OF SS304 STAINLESS STEEL: SIMULATION AND ITS FINITE ELEMENT ANALYSIS

Xiangjun Jiang

Xi'an Jiaotong University, Key Laboratory of Education Ministry for Modern Design and Rotor-Bearing System, Xi'an, PR China; e-mail: jxj97011311@yahoo.com.cn

Yongsheng Zhu

Xi'an Jiaotong University, Theory of Lubrication and Bearing Institute, Xi'an, PR China; e-mail: yszhu@mail.xjtu.edu.cn

Jun Hong

Xi'an Jiaotong University, State Key Laboratory for Manufacturing System, Xi'an, PR China
e-mail: jhong@mail.xjtu.edu.cn

Youyun Zhang

Xi'an Jiaotong University, Theory of Lubrication and Bearing Institute, Xi'an, PR China
e-mail: yyzhang1@mail.xjtu.edu.cn

Qianhua Kan

Southwest Jiaotong University, School of Mechanics and Engineering, Chengdu, PR China
e-mail: qianhuakan@yahoo.com.cn

Time-dependent ratchetting behaviour of SS304 stainless steel was experimentally conducted at room temperature and 973 K. The material shows distinct time-dependent deformation. However, under cyclic stressing with a certain peak/valley stress hold and at 973 K, more significant time-dependent inelastic behaviour was observed. Based on the Abdel-Karim-Ohno nonlinear kinematic hardening rule with the static recovery term, a time-dependent hardening rule incorporating an internal variable in the dynamic recovery term of the back stress is proposed to reasonably describe the evolution behaviour of time-dependent ratchetting with a certain peak/valley stress hold and at high temperature. Simultaneously, the proposed model is implemented into the ANSYS finite element package by User Programmable Features (UPFs). It is shown that the customized ANSYS model exhibits better performance than the reference model, especially under cyclic stressing with the certain peak/valley stress hold and at high temperature.

Key words: ratchetting, time-dependence, constitutive model, finite element method

1. Introduction

Fatigue failure is the final result of a complex microscopic phenomenon which occurs under cyclic loading. In structure components of a nuclear power system, the viscosity of the material and the time-dependence of ratchetting at high temperature, such as at 973 K, become as very remarkable, and should be addressed in detail. The time-independent and time-dependent deformation, caused by the slight opening of the hysteresis loop, can be reasonably described by some revised versions of the Armstrong-Fredrick non-linear kinematic hardening model (Abdel-Karim, 2005, 2010; Chaboche, 1991; Chen and Jia, 2004; Jiang and Sehitoglu, 1994; Kang and Gao, 2004; Kang *et al.*, 2002; McDowell, 1995; Ohno and Abdel-Karim, 2000; Yaguchi and Takahashi, 2005a,b). However, regarding the stress relaxation behaviour with a certain peak/valley stress hold under cyclic loading, few studies have been conducted so far. According to the creep-ratchetting experiments of SS304 stainless steel at room temperature and 973 K, the effects of stressing rate,

peak-stress hold and stress ratio on the ratchetting have been discussed by employing a unified visco-plastic model and a plasticity-creep superposition model (Mayama and Sasaki, 2006; Taleb and Cailletaud, 2011). A combined nonlinear kinematic hardening model with a static recovery term was firstly proposed by Chaboche (1977)] and extended by Kan *et al.* (2007) to describe the time-dependent ratchetting behaviour. It was shown that the unified visco-plastic model even employing the static recovery term cannot describe reasonably the creep-ratchetting behaviour especially at low stress ratios and high temperature. In order to provide an accurate simulation on the time-dependent ratchetting behaviour of the material more reasonably, it is necessary to develop a constitutive model to describe such remarkable time-dependent behaviour. The application of an advanced constitutive model into the finite element method is also indispensable to achieve an accurate stress-strain analysis for engineering structures. It was demonstrated that the ability to simulate structural ratchetting could be improved by implementing a more advanced constitutive model into ANSYS material library (ANSYS, 1995; Hassan etal, 1998; Kang, 2004, 2006; Kobayashi and Ohno, 2002; Rahman *et al.*, 2008).

In this work, a visco-plastic constitutive model with the static recovery term and the dynamic recovery term is proposed to describe the time-dependent ratchetting behaviour and to improve the capability of the models to simulate the interaction between creep and ratchetting. The capability of the proposed model is discussed by comparing with the corresponding experiments of the SS304 stainless steel material at room temperature and 973 K (Kang *et al.*, 2006). Simultaneously, the proposed model is successfully implemented into the finite element package ANSYS (1995). The corresponding consistent tangent operator is derived afresh by considering the influence of McCauley's bracket term.

2. Description of the constitutive models

In this work, the unified visco-plastic nonlinear kinematic hardening rule developed by Abdel-Karim and Ohno (simplified as UVP model hereafter) is employed as

$$\boldsymbol{\alpha}_{n+1} = \sum_{k=1}^{M} r^{(k)} \mathbf{b}_{n+1}^{(k)} \tag{2.1}$$

where $\boldsymbol{\alpha}$ is the total back stress which is divided into M components denoted as $\mathbf{b}^{(k)}$ multiply $r^{(k)}$ $(k = 1, 2, \ldots, M)$. The critical state of dynamic recovery is reflected by a surface

$$f^{(k)} = \overline{\alpha}^{(k)2} - r^{(k)2} = 0 \tag{2.2}$$

where $\overline{\alpha}^{(k)} = \sqrt{\frac{3}{2}\alpha^{(k)} : \alpha^{(k)}}$ is the equivalent back stress and $r^{(k)}$ is the radius of the critical surface.

Evaluation of the UVP model by Kan *et al.* (2007), Kang and Kan (2007) has demonstrated that this model was not robust enough to simulate the time-dependent ratchetting of the material at room and high temperature. Same as the evolution rule of the back stress using in the UVP model, a visco-plasticity-creep superposition constitutive model by employing a kinematic hardening rule with a static recovery term (simplified as MUVP I model) was proposed for simulation of creep or cyclic creep deformation. It could be found that the simulations were in good agreement with experiments (Kang and Kan, 2007), however, it should be noted that the superposition model is difficult to be directly implemented into finite element software. In this work, a modified Abdel-Karim and Ohno model (simplified as MUVP II model) with the additional dynamic recovery term of the back stress is introduced into the non-linear kinematic hardening term. Then the back stress evolution equation is expressed as

$$\dot{\mathbf{b}}^{(k)} = \frac{2}{3}\xi^{(k)}\dot{\boldsymbol{\varepsilon}}^{in} - \mathbf{Y}\dot{p} - \xi^{(k)}\Big[\mu^{(k)}\dot{p} + H(f^{(k)})\Big\langle \dot{\boldsymbol{\varepsilon}}^{in} : \frac{\boldsymbol{\alpha}^{(k)}}{r^{(k)}} - \mu^{(k)}\dot{p}\Big\rangle\Big]\mathbf{b}^{(k)} - \chi(\overline{\alpha}^{(k)})^{(m-1)}b^{(k)} \tag{2.3}$$

where $\xi^{(k)}$ and $r^{(k)}$ are temperature-dependent material parameters; (:) indicates the inner product between second-rank tensors; $H(f^{(k)})$ is the Heaviside function: if $f^{(k)} \geqslant 0$, $H(f^{(k)}) = 1$; $f^{(k)} < 0$, $H(f^{(k)}) = 0$, $p = \sqrt{\frac{2}{3}\varepsilon^{in} : \varepsilon^{in}}$ stands for accumulated inelastic strain, $\mu^{(k)}$ is a parameter allowing Eq. (2.3) to control the hysteresis loop with slight opening, if $0 < \mu^{(k)} \leqslant 1$. In this analysis, the ratchetting parameter $\mu^{(k)}$ is adopted identically for all the parts of back stress as μ. The static recovery term of the back stress, $-\chi(\overline{\alpha}^{(k)})^{(m-1)}$, is used to represent the time-dependent deformation with peak/valley stress hold, where χ and m are material constants. It can be determined by the trials-and-errors method from the uniaxial experimental ratchetting results. The second-rank tensor $\mathbf{Y}$ is the internal variable that was proposed and developed in Yaguchi *et al.* (2002a,b), Zhan and Tong (2007) to describe the evolutionary behaviour of the back stress with the dynamic recovery property. In the present study, the driving force of the variable $\mathbf{Y}$ is assumed to be time-dependent, and the evolution equation can be expressed as follows

$$\dot{\mathbf{Y}} = -\alpha'\{Y_{st}\,\mathrm{sgn}\,(\alpha^{(k)}) + \mathbf{Y}\}(\overline{\alpha}^{(k)})^{(m-1)} \tag{2.4}$$

Here α' and Y_{st} are material constants, α' describes the evolutionary rate of the variable $\mathbf{Y}$, and Y_{st} denotes the saturated value of $\mathbf{Y}$. The sgn function is defined as $\mathrm{sgn}\,(x) = 1$ if $x > 0$ and $\mathrm{sgn}\,(x) = -1$ if $x < 0$. The initial value of $\mathbf{Y}$ is taken to be zero, and the constants α' and Y_{st} are assumed to be positive and can be determined by the trails-and-errors method at certain temperature.

3. Finite element model

The finite element model should represent the central part of the specimen where stresses can be assumed to be uniform. A 3D eight-noded solid185 brick element is employed for calculating the uniaxial time-dependent ratchetting behaviour of the material. Additionally, an axi-symmetrical notched-bar subjected to the uniaxial cyclic stressing with non-zero mean stress is discussed. A 2D axi-symmetrical four-noded plane182 element mesh is employed to set up the finite element model for the notched-bar (Kan *et al.*, 2007). Detailed formulation for the implementation of the material model is presented in Appendix A. The material parameters are the same as those used in constitutive simulation and are listed in Tables 1 and 2.

Table 1. Material constants for all models at two temperatures

$M = 8$, room temperature				
$\xi^{(1)} = 3341$	$\xi^{(2)} = 1833$	$\xi^{(3)} = 765.6$	$\xi^{(4)} = 210.4$	
$\xi^{(5)} = 69.92$	$\xi^{(6)} = 35.91$	$\xi^{(7)} = 23.04$	$\xi^{(8)} = 13.0$	
$r^{(1)} = 37.85$	$r^{(2)} = 34.56$	$r^{(3)} = 18.89$	$r^{(4)} = 11.92$	
$r^{(5)} = 8.38$	$r^{(6)} = 6.74$	$r^{(7)} = 12.41$	$r^{(8)} = 70.33$	
$E = 192\,\mathrm{GPa}$	$\nu = 0.33$	$K = 72$	$n = 15$	$Q_0 = 90$
$M = 8$, at 973 K				
$\xi^{(1)} = 3306$	$\xi^{(2)} = 1703$	$\xi^{(3)} = 726.7$	$\xi^{(4)} = 208.5$	
$\xi^{(5)} = 69.35$	$\xi^{(6)} = 36.15$	$\xi^{(7)} = 22.94$	$\xi^{(8)} = 13$	
$r^{(1)} = 12.16$	$r^{(2)} = 14.14$	$r^{(3)} = 13.19$	$r^{(4)} = 3.76$	
$r^{(5)} = 7.86$	$r^{(6)} = 16.08$	$r^{(7)} = 7.91$	$r^{(8)} = 24.01$	
$E = 125\,\mathrm{GPa}$	$\nu = 0.33$	$K = 35$	$n = 9$	$Q_0 = 48$

Table 2. Correlation coefficients for the parameters of the models

	At room temperature			At 973 K		
	UVP	MUVP I	MUVP II	UVP	MUVP I	MUVP II
μ	0.04	0.03	0.05	0.035	0.01	0.01
χ	0	5E-13	0	0	1.7E-9	2.43E-9
m	0	5	0	0	4.5	4.54
Y_{st}	0	0	30	0	0	8
α'	0	0	3E-16	0	0	6.55E-13

4. Simulations and results

The previous experimental results firstly conducted by Kan *et al.* (2007) are used to evaluate the performance of non-linear kinematic hardening rules with finite element application in this work. In addition, temperature-dependent material parameters for the proposed model are obtained from the uniaxial tensile response. The material constants E, ν, K, n, $\xi^{(k)}$, $r^{(k)}$, Q_0 can be determined by the procedure described in the previous work (Kang *et al.*, 2006) shown in Tables 1 and 2. The cnstants χ, m and α' can be determined from the cyclic stress-strain curve with peak/valley stress hold by the trials-and-errors method at certain temperature. The uniaxial ratchetting behaviour of SS304 stainless steel with constant or variable stress rates are simulated numerically by the visco-plastic constitutive model mentioned in this paper. The simulation results are shown in Figs. 1, 2, 3b,c, 4, 5b,c for different loading conditions, respectively. In these simulations, a constant $m = 8$ is applied for all components of the back stress.

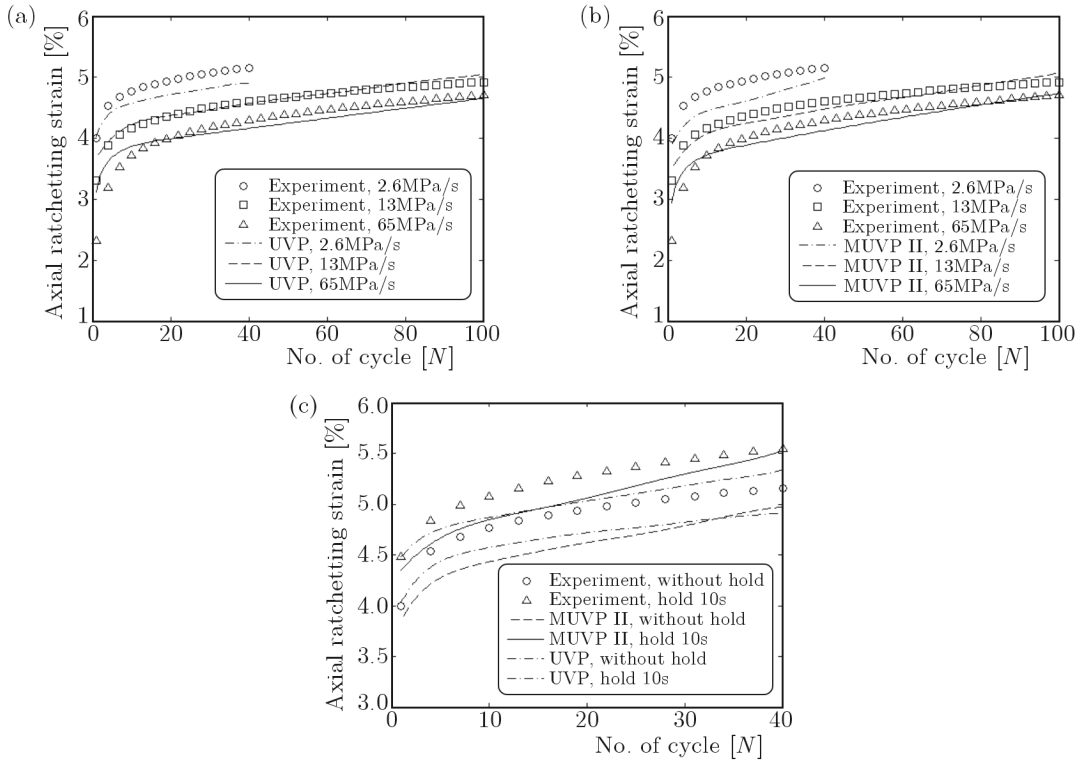

Fig. 1. (a) Simulation by the UVP model for different rates and at room temperature; (b) simulation by MUVP II ($\chi = 0$) model for different rates and at room temperature; (c) simulation by MUVP II ($\chi = 0$) model with or without peak/valley stress hold and at room temperature and stressing rate of 2.6 MPa/s

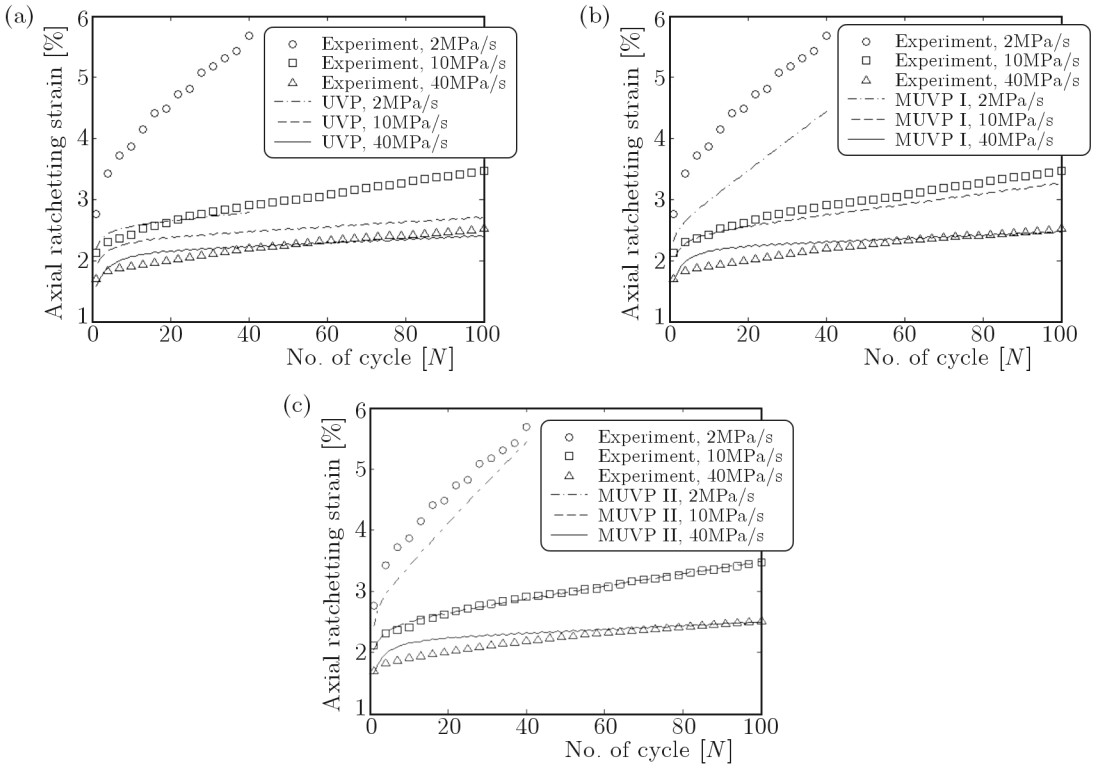

Fig. 2. Results of uniaxial ratchetting strain vs. cyclic number for different rates and at 973 K: (a) simulations by UVP model; (b) simulations by MUVP I model; (c) simulations by MUVP II model

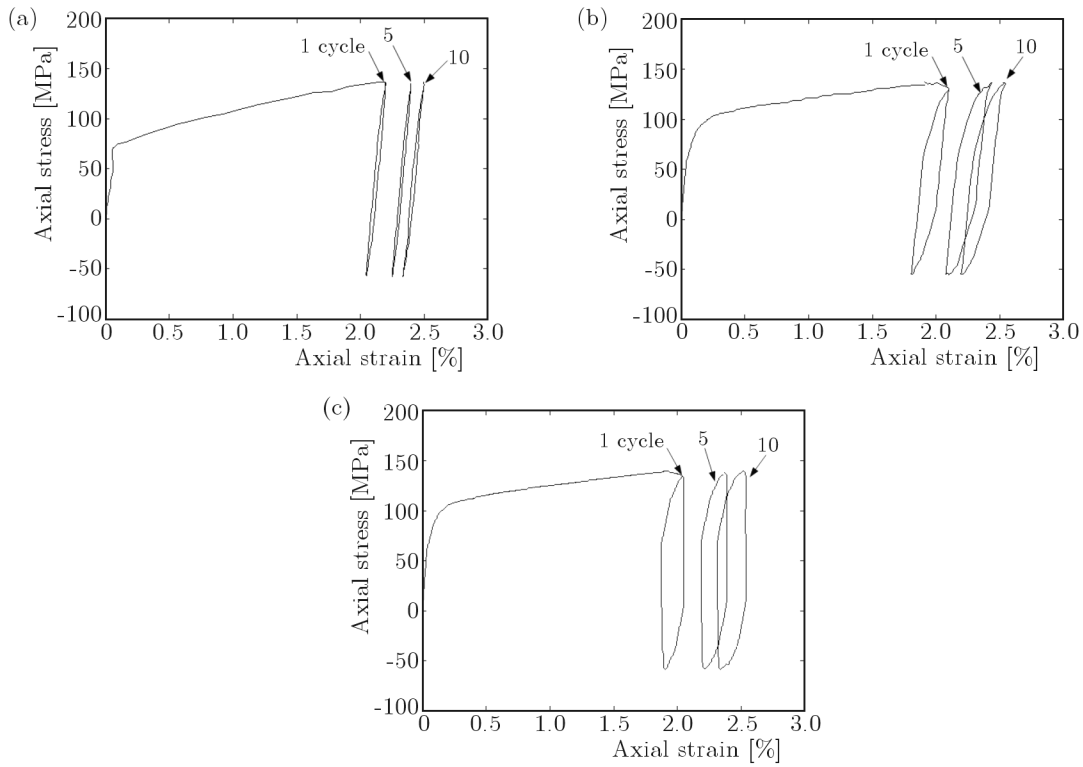

Fig. 3. Results of uniaxial ratchetting (40 ± 100 MPa) at 973 K and stressing rate of 10 MPa/s: (a) experiment; (b) simulation by ANSYS with the MUVP II model; (c) simulation of ratchetting for the notched-bar by the MUVP II model

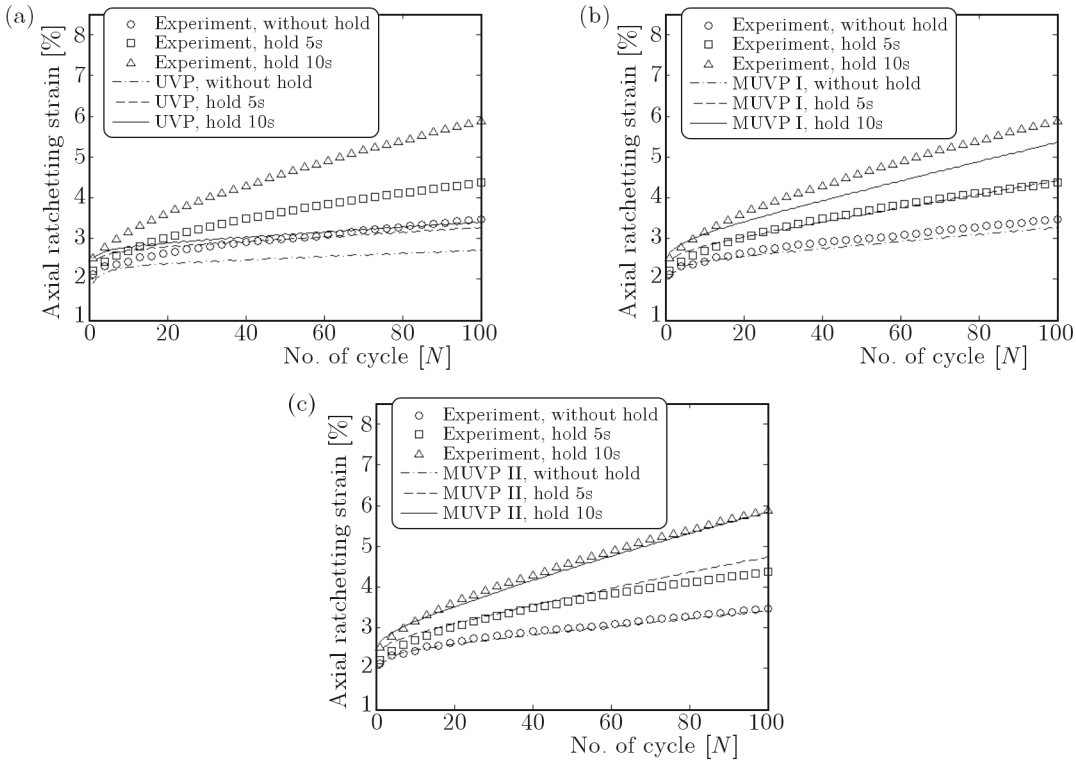

Fig. 4. Results of uniaxial ratchetting strain vs. cyclic number with or without peak/valley stress hold at 973 K and stressing rate of 10 MPa/s: (a) simulations by the UVP model; (b) simulations by the MUVP I model; (c) simulations by the MUVP II model

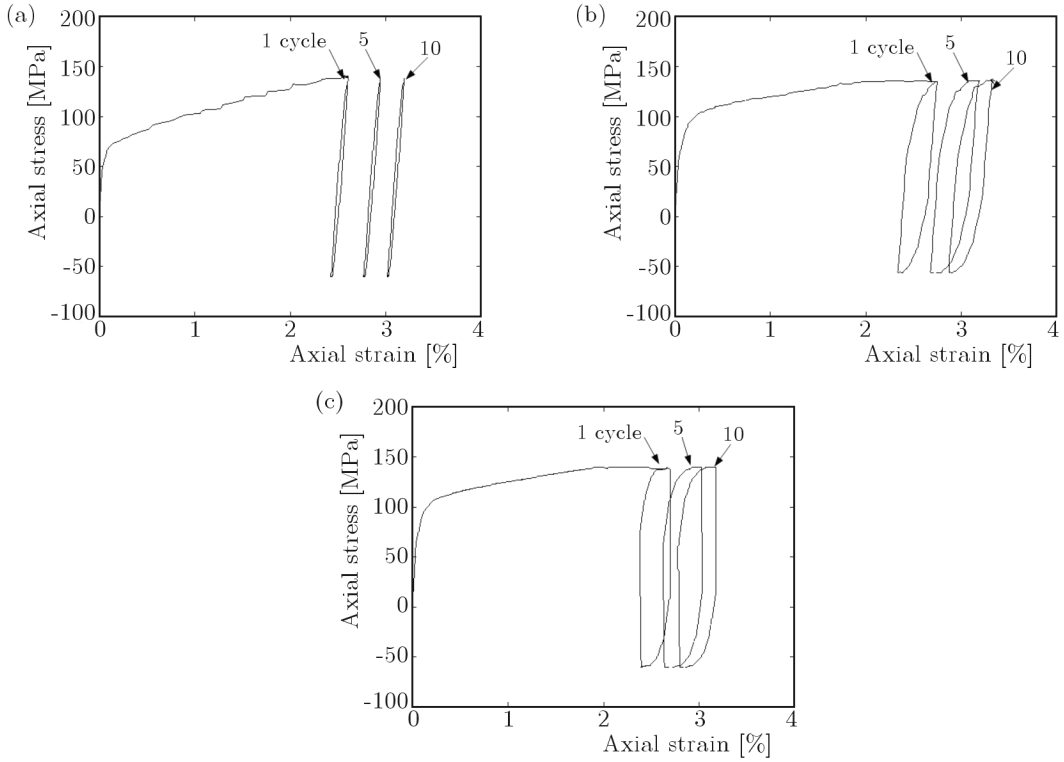

Fig. 5. Results of ratchetting (40 ± 100 MPa) with peak/valley stress hold at 973 K and stressing rate of 10 MPa/s: (a) experiment; (b) simulation by ANSYS with the MUVP II model; (c) simulation of ratchetting for the notched-bar by the MUVP II model

From the experimental and simulated ratchetting results at room temperature shown in Figs. 1, it can be concluded that: (1) the UVP model can provide good simulations for the uniaxial ratchetting of the material at moderate stressing rates, such as at 65 MPa/s and 13 MPa/s, however, at a lower stressing rate, i.e., 2.6 MPa/s, the simulation by this model shows a larger divergence from the corresponding experiments; (2) the UVP model has the capability of simulating the variation of ratchetting strain caused by the varied hold-times at peak/valley stress points reasonably, though it cannot well simulate the time-dependent ratchetting behaviour of the material at lower stressing rate well; (3) though the improvement at varied stressing rates and varied hold-times at peak/valley stress points could be obtained by using the MUVP I model proposed in Kan *et al.* (2007), the MUVP II model with the dynamic recovery term only provides more reasonable simulations for the time-dependent ratchetting behaviour of the material compared with the UVP model for varied hold-times at peak/valley stress points.

The experiments and simulations at 973 K are shown in Figs. 2, 3, 4 and 5. It can be concluded that: (1) since the viscosity of the material is very remarkable at 973 K, the UVP model cannot provide good simulations for the time-dependent ratchetting of the material, even at moderate stressing rates, such as at 40 MPa/s and 10 MPa/s, and for those with various hold-times at peak/valley stress points, as shown in Figs. 2a and 4a; (2) although the MUVP I model can provide good simulations for the time-dependent ratchetting behaviour of the material presented at varied stressing rates and with different hold-times at room temperature, it cannot simulate the time-dependent ratchetting at lower stressing rates as shown in Fig. 2b. Moreover, the MUVP I model cannot describe the ratchetting strain by various hold-times precisely as can be seen in Fig. 3b, since the static recovery term only adopted in this model cannot reasonably take this effect into account at lower stressing rates; (3) compared with the simulation results by the MUVP I model, the MUVP II model can provide good simulations for the time-dependent ratchetting behaviour of the material presented at varied stressing rates and hold-times at 973 K, as shown in Figs. 2c and 4c; (4) similar to that at room temperature, the customized ANSYS model based on the MUVP II model can provide reasonable simulations for the time-dependent ratchetting behaviour of the material presented at 973 K, as shown in Figs. 3b,c and 5b,c. Nevertheless, it should be noted that at 973 K, owning to the simulations by this model mainly focused on the value of time-dependent ratchetting strain, the predicted shape of stress-strain hysteresis loop apparently deviates from the experimental one even with the MUVP II model, which should be improved in the further work.

5. Conclusions

Based on the time-dependent deformation characteristics observed from experimental results obtained by Kang *et al.* (2006), three types of constitutive models are employed to simulate the uniaxial time-dependent ratchetting of SS304 stainless steel at room temperature and 973 K. It is shown from the above discussions that the proposed visco-plastic constitutive model is reasonably formulated by the unified visco-plastic constitutive model rule with the static and dynamic recovery term. The simulation results found through the proposed model are in good consistence with the experimental results of the uniaxial time-dependent ratchetting of SS304 stainless steel at room temperature and 973 K. Finally, the customized ANSYS model has demonstrated that it is capable of simulating the time-dependent ratchetting deformation accurately for some structures at room and even high temperatures with a certain peak stress hold.

A. Appendix

The plasticity model discussed in Section 3 is implemented into the general purpose FE package ANSYS through the user-defined subroutine USERMAT. A new explicit stress update algori-

thm and the corresponding consistent tangent operator are derived based on backward Euler algorithm and radial return method. The algorithm reduces the plasticity model into a nonlinear equation that can be solved by Newton's method.

The discretized evolution rules of kinematic hardening are given by

$$\alpha_{n+1} = \sum_{k=1}^{M} r^{(k)} b_{n+1}^{(k)} \tag{A.1}$$

— for MUVP I

$$\dot{\mathbf{b}}^{(k)} = \frac{2}{3}\xi^{(k)}\dot{\boldsymbol{\varepsilon}}^{in} - \xi^{(k)}\Big[\mu^{(k)}\dot{p} + H(f^{(k)})\Big\langle \dot{\boldsymbol{\varepsilon}}^{in} : \frac{\boldsymbol{\alpha}^{(k)}}{r^{(k)}} - \mu^{(k)}\dot{p}\Big\rangle\Big]\mathbf{b}^{(k)} - \chi(\overline{\alpha}_{n+1}^{(k)})^{(m-1)}\mathbf{b}_{n+1}^{(k)} \tag{A.2}$$

— for MUVP II

$$\dot{\mathbf{b}}^{(k)} = \frac{2}{3}\xi^{(k)}\dot{\boldsymbol{\varepsilon}}^{in} - \mathbf{Y}\dot{p} - \xi^{(k)}\Big[\mu^{(k)}\dot{p} + H(f^{(k)})\Big\langle \dot{\boldsymbol{\varepsilon}}^{in} : \frac{\boldsymbol{\alpha}^{(k)}}{r^{(k)}} - \mu^{(k)}\dot{p}\Big\rangle\Big]\mathbf{b}^{(k)} - \chi(\overline{\alpha}_{n+1}^{(k)})^{(m-1)}\mathbf{b}_{n+1}^{(k)} \tag{A.3}$$

and

$$\mathbf{b}_{n+1}^{(k)} = \theta_{n+1}^{(k)}\mathbf{b}_{n+1}^{*(k)} \tag{A.4}$$

where, if $\Delta\boldsymbol{\varepsilon}_{n+1}^{in}:\ \mathbf{b}_{n+1}^{(k)} - \mu^{(k)}\Delta p_{n+1} > 0$ and $H(f^{(k)}) = 1$ then

$$\theta_{n+1}^{(k)} = \frac{1}{1 + \mu^{(k)}\xi^{(k)}\Delta p_{n+1} + \xi^{(k)}(\Delta\boldsymbol{\varepsilon}_{n+1}^{in} : \mathbf{b}_{n+1}^{(k)} - \mu^{(k)}\Delta p_{n+1}) + \chi(r^{(k)}\overline{b}_{n+1}^{(k)})^{(m-1)}\mathbf{b}_{n+1}^{(k)}} \tag{A.5}$$

otherwise

$$\theta_{n+1}^{(k)} = \frac{1}{1 + \mu^{(k)}\xi^{(k)}\Delta p_{n+1} + \chi(r^{(k)}\overline{b}_{n+1}^{(k)})^{(m-1)}\mathbf{b}_{n+1}^{(k)}} \tag{A.6}$$

and

$$\mathbf{b}_{n+1}^{*(k)} = \begin{cases} \mathbf{b}_{n}^{(k)} + \dfrac{2}{3}\xi^{(k)}\Delta\boldsymbol{\varepsilon}_{n+1}^{in} & \text{for MUVP I} \\ (A.7)\mathbf{b}_{n}^{(k)} + \dfrac{2}{3}\xi^{(k)}\Delta\boldsymbol{\varepsilon}_{n+1}^{in} - \mathbf{Y}_{n+1}\Delta p_{n+1} & \text{for MUVP II} \end{cases} \tag{A.7}$$

as done by ANSYS (1995), Yaguchi *et al.* (2002b), Zhan and Tong (2007), a new nonlinear scalar equation of stress integration for the proposed model is obtained as

$$\overline{Y}_{n+1} - \overline{Y}_{n+1}^{*} + \left(3G + \sum_{i=1}^{m}\theta_{n+1}^{(k)}\xi^{(k)}r^{(k)}\right)\Big\langle\frac{\overline{Y}_{n+1} - Q_0}{K}\Big\rangle^{n}\Delta t_{n+1} = 0 \tag{A.8}$$

where

$$\overline{Y}_{n+1} = \sqrt{\frac{3}{2}}\|s_{n+1} - \alpha_{n+1}\| \qquad \overline{Y}_{n+1}^{*} = \sqrt{\frac{3}{2}}\left\|\mathbf{s}_{n+1}^{*} - \sum_{i=1}^{m} r^{(k)}\theta_{n+1}^{(k)}\mathbf{b}_{n}^{(k)}\right\| \tag{A.9}$$

where $\mathbf{s}_{n+1}^{*}$ is the elastic predictor of deviatoric stress $\mathbf{s}_{n+1}$, and $\mathbf{b}_{n+1}^{*(k)}$ is the predictor of $\dot{\mathbf{b}}_{n+1}^{(k)}$. The stress and internal variables are determined in the iteration process, while the last subsection is convergent. If the equilibrium for the global FE equations is satisfied, the solution

is validated. Then, a new global equilibrium iteration is required. The consistent tangential modulus $d\Delta\boldsymbol{\sigma}_{n+1}/d\Delta\boldsymbol{\varepsilon}_{n+1}$ should be determined to ensure quadric convergence. This consistent tangential matrix can be derived for the proposed constitutive model as

$$\frac{d\Delta\boldsymbol{\sigma}_{n+1}}{d\Delta\boldsymbol{\varepsilon}_{n+1}} = \mathbf{D} - 4G^2(\mathbf{L}_{n+1}^{-1} : \mathbf{J}_{n+1}^{0}) : \mathbf{I}_d \tag{A.10}$$

where $\mathbf{D}$ is the fourth-order elasticity tensor.

This is similar to that obtained by ANSYS (1995), Yaguchi *et al.* (2002b), Zhan and Tong (2007) in form, but

$$\mathbf{L}_{n+1}^{(k)} = \mathbf{I} + \mathbf{J}_{n+1}^{0} : (2G\mathbf{I} + \mathbf{b}_{n+1}^{(k)} \otimes \mathbf{b}_{n+1}^{(k)}) \tag{A.11}$$

where

$$\begin{aligned}
&\mathbf{J}_{n+1}^{0} = \frac{3}{2}A(\mathbf{n}_{n+1}^{0} \otimes \mathbf{n}_{n+1}) + \sqrt{\frac{3}{2}}\Delta p_{n+1}\mathbf{J}_{n+1} \\
&\mathbf{n}_{n+1}^{0} = \mathbf{n}_{n+1} + \Delta p_{n+1}\mathbf{J}_{n+1} : \mathbf{b}'_{n+1} \\
&\mathbf{J}_{n+1} = \frac{1}{\|\mathbf{s}_{n+1} - \boldsymbol{\alpha}_{n+1}\|}(\mathbf{I} - \mathbf{n}_{n+1} \otimes \mathbf{n}_{n+1}) \\
&d\Delta p_{n+1} = A\sqrt{\frac{3}{2}}\mathbf{n}_{n+1} : \left[2G\mathbf{I}_d : d\Delta\boldsymbol{\varepsilon}_{n+1} - \left(2G\mathbf{I} + \sum_{i=1}^{m}\mathbf{H}_{n+1}^{(k)}\right) : d\Delta\boldsymbol{\varepsilon}_{n+1}^{in}\right] \\
&A = \frac{n(\Delta t_{n+1}/K)\langle F_{y(n+1)}/K\rangle^{n-1}}{1 + n(\Delta t_{n+1}/K)\langle F_{y(n+1)}/K\rangle^{n-1}(\mathbf{n}_{n+1} : \mathbf{b}'_{n+1})}
\end{aligned} \tag{A.12}$$

where, if $\Delta\boldsymbol{\varepsilon}_{n+1}^{in} : \mathbf{b}_{n+1}^{(k)} - \mu^{(k)}\Delta p_{n+1} > 0$ and $H(f^{(k)}) = 1$ then

$$\begin{aligned}
&\mathbf{b}'_{n+1} = \mathbf{0} \qquad \mathbf{H}_{n+1}^{(k)} = \theta_{n+1}^{(k)}\xi^{(k)}r^{(k)}\mathbf{M}_{n+1}^{(k)^{-1}} : \left(\frac{2}{3}\mathbf{I} - \mathbf{b}_{n+1}^{(k)} \otimes \mathbf{b}_{n+1}^{(k)}\right) \\
&\mathbf{M}_{n+1}^{(k)} = \mathbf{I} + \theta_{n+1}^{(k)}\xi^{(k)}\mathbf{b}_{n+1}^{(k)} \otimes \Delta\boldsymbol{\varepsilon}_{n+1}^{in} + (m-1)\theta_{n+1}^{(k)}\chi r^{(k)(m-1)}\overline{b}_{n+1}^{(k)(m-3)}\mathbf{b}_{n+1}^{(k)} \otimes \mathbf{b}_{n+1}^{(k)}
\end{aligned} \tag{A.13}$$

otherwise

$$\begin{aligned}
&\mathbf{b}'_{n+1} = \sum_{i=1}^{M}(-1)\theta_{n+1}^{(k)}\xi^{(k)}r^{(k)}\mu^{(k)}\mathbf{M}_{n+1}^{(k)^{-1}} : \mathbf{b}_{n+1}^{(k)} \\
&\mathbf{H}_{n+1}^{(k)} = \theta_{n+1}^{(k)}\xi^{(k)}r^{(k)}\mathbf{M}_{n+1}^{(k)^{-1}} : \left(\frac{2}{3}\mathbf{I} - \mathbf{b}_{n+1}^{(k)} \otimes \mathbf{b}_{n+1}^{(k)}\right) \\
&\mathbf{M}_{n+1}^{(k)} = \mathbf{I} + (m-1)\theta_{n+1}^{(k)}\chi r^{(k)(m-1)}\overline{b}_{n+1}^{(k)(m-3)}\mathbf{b}_{n+1}^{(k)} \otimes \mathbf{b}_{n+1}^{(k)}
\end{aligned} \tag{A.14}$$

the symbol $\otimes$ represents the dyadic tensor product, (:) stands for tensor contraction, and $\mathbf{I}$ is the fourth order unit tensor, $\mathbf{I}_d = \left(\mathbf{I} - \frac{1}{3}\mathbf{1} \otimes \mathbf{1}\right)$ represents the deviatoric operation of a tensor, $\mathbf{1}$ is a second-order unit tensor.

Acknowledgments

We would like to thank for the financial support of this work by the National Basic Research Program of China (Grant No. 2011CB706601) and the key project of National Natural Science Foundation of China (No. 50935006).

References

1. Abdel-Karim M., 2005, Numerical integration method for kinematic hardening rules with partial activation of dynamic recovery term, *International Journal of Plasticity*, **21**, 1303-1321

2. Abdel-Karim M., 2010, An evaluation for several kinematic hardening rules on prediction of multiaxial stress-controlled ratchetting, *International Journal of Plasticity*, **26**, 711-730

3. ANSYS Release 5.1, 1995, Swanson Analysis System, Inc., Houston, PA 15342

4. Chaboche J.L., 1977, Viscoplastic constitutive equations for description of cyclic and anisotropic behaviour of metals, *Bulletin De L Academie Polonaise Des Sciences-Serie Des Sciences Techniques*, **25**, 39-48

5. Chaboche J.L., 1991, On some modifications of kinematic hardening to improve the description of ratchetting effects, *International Journal of Plasticity*, **7**, 661-678

6. Chen X., Jiao R., 2004, Modified kinematic hardening rule for multiaxial ratchetting prediction, *International Journal of Plasticity*, **20**, 871-898

7. Hassan T., Zhu Y., Matzen V.C., 1998, Improved ratchetting analysis of piping components, *International Journal of Pressure Vessels and Piping*, **75**, 643-652

8. Jiang Y.Y., Sehitoglu H., 1994, Cyclic ratchetting of 1070 steel under multiaxial stress states, *International Journal of Plasticity*, **10**, 579-608

9. Kan Q.H., Kang G.Z., Zhang J., 2007, Uniaxial time-dependent ratchetting: Visco-plastic model and finite element application, *Theoretical and Applied Fracture Mechanics*, **47**, 133-144

10. Kang G.Z., 2004, A visco-plastic constitutive model for ratchetting of cyclically stable materials and its finite element implementation, *Mechanics of Materials*, **36**, 299-312

11. Kang G.Z., 2006, Finite element implementation of visco-plastic constitutive model with strain-range-dependent cyclic hardening, *Communications in Numerical Methods in Engineering*, **22**, 137-153

12. Kang G.Z., Gao Q., 2004, Temperature-dependent cyclic deformation of SS304 stainless steel under non-proportionally multiaxial load and its constitutive modeling, *Advances in Engineering Plasticity and Its Applications, Pts 1 and 2*, 274-276, 247-252

13. Kang G.Z., Gao Q., Yang X.J., 2002, A visco-plastic constitutive model incorporated with cyclic hardening for uniaxial/multiaxial ratchetting of SS304 stainless steel at room temperature, *Mechanics of Materials*, **34**, 521-531

14. Kang G.Z., Kan Q.H., 2007, Constitutive modeling for uniaxial time-dependent ratcheting of SS304 stainless steel, *Mechanics of Materials*, **39**, 488-499

15. Kang G.Z., Kan Q.H., Zhang J., 2006, Time-dependent ratchetting experiments of SS304 stainless steel, *International Journal of Plasticity*, **22**, 858-894

16. Kobayashi M., Ohno N., 2002, Implementation of cyclic plasticity models based on a general form of kinematic hardening, *International Journal for Numerical Methods in Engineering*, **53**, 2217-2238

17. Mayama T., Sasaki K., 2006, Investigation of subsequent viscoplastic deformation of austenitic stainless steel subjected to cyclic preloading, *International Journal of Plasticity*, **22**, 374-390

18. McDowell D.L., 1995, Stress state dependence of cyclic ratchetting behaviour of two rail steels, *International Journal of Plasticity*, **11**, 397-421

19. Ohno N., Abdel-Karim M., 2000, Uniaxial ratchetting of 316FR steel at room temperature-Part II: Constitutive modeling and simulation, *ASME Journal of Engineering Materials and Technology*, **122**, 35-41

20. Rahman S.M., Hassan T., Corona E., 2008, Evaluation of cyclic plasticity models in ratchetting simulation of straight pipes under cyclic bending and steady internal pressure, *International Journal of Plasticity*, **24**, 1756-1791

21. Taleb L., Cailletaud G., 2011, Cyclic accumulation of the inelastic strain in the 304L SS under stress control at room temperature: Ratcheting or creep?, *International Journal of Plasticity*, In Press, Corrected Proof

22. Yaguchi M., Takahashi Y., 2005a, Ratchetting of viscoplastic material with cyclic softening: I. Experiments on modified 9Cr-1Mo steel, *International Journal of Plasticity*, **21**, 43-65

23. Yaguchi M., Takahashi Y., 2005b, Ratchetting of viscoplastic material with cyclic softening: II. Application of constitutive models, *International Journal of Plasticity*, **21**, 835-860

24. Yaguchi M., Yamamoto M., Ogata T., 2002a, A viscoplastic constitutive model for nickel-base superalloy, part 1: kinematic hardening rule of anisotropic dynamic recovery, *International Journal of Plasticity*, **18**, 1083-1109

25. Yaguchi M., Yamamoto M., Ogata T., 2002b, A viscoplastic constitutive model for nickel-base superalloy, part 2: modeling under anisothermal conditions, *International Journal of Plasticity*, **18**, 1111-1131

26. Zhan Z.L., Tong J., 2007, A study of cyclic plasticity and viscoplasticity in a new nickel-based superalloy using unified constitutive equations. Part II: Simulation of cyclic stress relaxation, *Mechanics of Materials*, **39**, 73-80

Konstytutywny model zależnego od czasu zjawiska ratchetingu dla stali SS304 – symulacja i analiza metodą elementów skończonych

Streszczenie

W pracy przedstawiono wyniki badań eksperymentalnych nad zależnym od czasu procesem zmęczeniowym typu ratcheting przeprowadzonych w temperaturze pokojowej oraz podwyższonej do 973 K. Materiał wykazał wyraźnie zależną od czasu funkcję deformacji. Podczas cyklicznego obciążania przy zadanych wartościach min/max naprężeń w temperaturze 973 K zaobserwowano silnie nieliniowe i zależne od czasu zachowanie się badanej stali. Do wyjaśnienia tego zjawiska, zwanego ratchetingiem zależnym od czasu, wykorzystano model umocnienia materiału oparty na nieliniowej formule kinematycznego umocnienia Abdela-Karima-Ohno ze statycznym członem odprężania. Model ten zmodyfikowano, wprowadzając wewnętrzną zmienną w dynamicznym członie odprężania przy obciążeniu powrotnym. Jednocześnie zaproponowany model wdrożono do systemu ANSYS poprzez zastosowanie pakietu *User Programmable Features* (UPFs). Wykazano, że taka modyfikacja systemu ANSYS charakteryzuje się lepszym działaniem w stosunku do standardowego oprogramowania. Jest to szczególnie zauważalne dla symulacji cyklicznego obciążenia stali w podwyższonej temperaturze.

Manuscript received December 15, 2011; accepted for print March 15, 2012